Original Article
MicroRNA expression profiling of kidney tissues in patients with congenital ureteropelvic junction obstruction

Wenzong Gao[1], Yi Zhou[2], Juntao Xie[1], Zhe Xu[1], Li Zhou[1]

Departments of [1]Pediatric Surgery, [2]Fetal Medical Center, First Affiliated Hospital, University of Sun Yat-sen, Guangzhou, Guangdong, China

Abstract: Objectives: To identify microRNA expression signature in patients with congenital ureteropelvic junction obstruction (UPJO) compared with normal kidney tissues, and explore microRNAs that have a relationship with the renal function of patients with congenital hydronephrosis. Methods: A total of four patients with UPJO were recruited into this study in The First Affiliated Hospital of Sun Yet-sen University. The case group samples were harvested from patients with congenital UPJO, while the control group samples were normal kidney tissues adjacent to tumors harvested from patients with nephroblastoma. MiRNA expression profiles were assessed using miRNA microarrays. The target genes and the functions of selected microRNA were analyzed using bioinformatic methods. Results: Five miRNAs were significantly altered in patients with congenital UPJO with the control group. Bioinformatic analyses of these differentially expressed miRNAs showed that three up-regulated miRNAs were associated with each other through a protein-protein interaction (PPI) sub-network. In addition, enrichment analyses showed that most of the genes targeted by the three up-regulated miRNAs were associated with tumor apoptosis. Conclusions: Our analysis showed that miRNA expression profiling of kidney tissues are altered in congenital UPJO patients which may contribute to the disease progression through different biological processes. After proper validation, these microRNAs may play significant roles in the therapeutic applications and be the potential therapeutic targets in congenital UPJO.

Keywords: MicroRNA, microarray, congenital ureteropelvic junction obstruction (UPJO), expression profiling, Akt/mTOR pathway

Introduction

Congenital hydronephrosis is a renal urinary disease characterized by distension and dilation of the renal pelvis with an overall prevalence of 11.5 cases per 10,000 births [1, 2]. Ureteralpelvic junction obstruction (UPJO) is the primary cause of obstructive nephropathy. Therapeutic approaches for treatment of this disease vary based on the severity of hydronephrosis. The pathologic evolution of obstructive nephropathy is an overlapping sequence of cellular events, including tubular dilatation, phenotypic cellular transition, cell death and interstitial inflammation, following by glomerulo-tubular injury and progressive interstitial fibrosis [1]. Mild hydronephrosis may require only observation, while operative intervention is necessary for children having severe hydronephrosis. However, the timing of surgery is still controversial. In clinics, ultrasound (US), computerized tomography (CT), magnetic resonance imaging (MRI) and diuretic renal flow scan (RFS) are normally used to assess the severity of hydronephrosis. However, these methods can hardly used for accurate characterization of the damage and loss of renal function, measure of the renal function reserve, or prediction of the eventual outcome [3]. Therefore, the development of effective therapeutic methods for evaluating the severity of hydronephrosis depending on biomarkers is necessary to prevent irreversible renal dysfunction [4]. Such biomarkers should ideally be correlated with renal injury or disease progression [5].

MicroRNAs (miRNAs) are a class of endogenous short non-coding RNAs that play important roles in cell function and development through
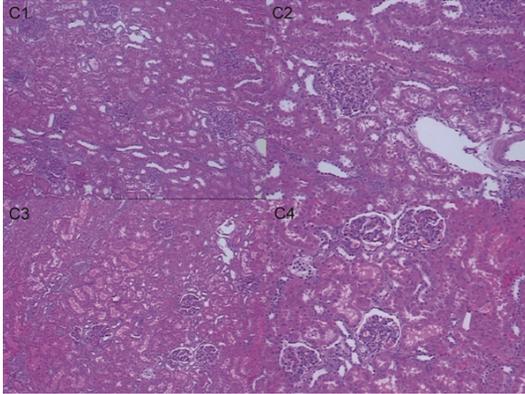
Figure 1. Kidney tissue structures in the control groups under light microscope (×100). C1-4 represents four subjects enrolled in the control groups.

targeting and silencing of mRNA sequences. They have a critical role as regulator by controlling many cellular and physiological activities in cell cycle, growth, proliferation, apoptosis and metabolism [6]. MiRNA expression profiles have been suggested to be a promising panel of biomarkers that can help elucidate tumor diagnosis, prognosis, prevention or treatment.

Both *in vitro* and *in vivo* animal models have shown a critical role of miRNAs in the process of renal dysfunction. In a mouse model of unilateral ureteral obstruction (UUO), mir-192 was found highly up-regulated [7]. In a rat model of UUO, Denby et al. [8] found that mir-21 and mir-214 are up-regulated, while Qin et al. [9] found that mir-29 is up-regulated in wild mice with UUO. Similarly, in another mouse model of UUO, Oba et al. [10] found that mir-200 family is up-regulated in a time-dependent manner, with the induction of mir-200b being most pronounced. In another murine model, Xiong et al. [11] found that the mir-200 family is down-regulated. Kriegel et al. [12] found that the expression of mir-382 in the obstructed kidneys of mice increased several fold compared with sham-operated controls, and Zarjou et al. found that mir-21 shows the greatest increase in the kidneys of mice with UUO. Bai et al. [13] confirmed that the expression of miRNA in the same organs differs according to age. Together, these studies provide evidence of the importance of microRNAs in renal function and dysfunction, although these biomarkers of hydronephrosis vary based on the difference of tissue source or developmental stage of the kidney. To our knowledge, there has been no study investigating the microRNA expression profile of UPJO in children.

In the present study, a miRNA microarray was performed to analyze the genome-wide miRNA expression profiling in UPJO and normal kidney tissues. We hypothesized that some miRNAs may play an important role in the process of UPJO and may serve as diagnostic biomarkers to identify UPJO in children, serving as reliable diagnostic markers and potential therapeutic targets.

Materials and methods

Study population and tissue collection

Four samples in the experimental group, with split renal function lower than 40%, were collected from the patients admitted to the pediatric surgical unit of The First Affiliated Hospital of Sun Yet-sen University during January 2011 and December 2012. Normal kidney tissues were harvested from human nephrectomy specimens removed from patients with nephroblastoma [14]. Four boys were enrolled in the control group aged 6 to 13 months. The 4 samples for control group were renal cortex got from resection operation of renal tumor which located far from tumor tissue and tissue structures were normal through light microscope checking (**Figure 1**).

The parents of all the patients were informed about this study and voluntarily joined this study after signing informed consents. This study was approved by the Medical Ethics Committee of our hospital.

Microarray

Microarray experiments were carried out on the 6th generation of miRCURYTM LNA Array (v.16.0) (Exiqon, Vedbaek, Denmark) contains more than 1,891 capture probes, covering all human, mouse and rat microRNAs annotated in miR-Base 16.0, as well as all viral microRNAs related to these species. In addition, this array contains capture probes for 66 new miRPlusTM human microRNAs.

RNA extraction

In brief, total RNA was isolated from the individual tissues using TRIzol (Invitrogen, Carlsbad, CA) and miRNeasy mini kit (QIAGEN, Hilden,

Table 1. Baseline characteristics and RNA quality of samples

Sample*	Age (month)	Split renal function (%)	OD260/280	OD260/230	Conc. (ng/μl)	Volume (μl)	Quantity (ng)
T1	8	35.64%	2.00	2.32	1087.92	25	27198.00
T2	20	37.83%	1.94	2.19	740.82	25	18520.50
T3	14	38.77%	2.02	2.08	628.20	30	18846.00
T4	17	33.41%	2.05	2.14	902.67	40	36106.80
C1			2.01	1.94	937.79	30	28133.70
C2			1.99	2.13	869.79	40	34791.60
C3			2.04	1.90	1025.18	60	61510.80
C4			2.02	2.13	782.07	50	39109.50

For spectrophotometer, the O.D. A260/A280 ratio should be close to 2.0 for pure RNA (ratios between 1.8 and 2.1 are acceptable). The O.D. A260/A230 ratio should be more than 1.8. *T: the experimental group; C: the control group.

Germany) according to manufacturer's instructions, which efficiently recovered all RNA species, including miRNAs. RNA quality and quantity was determined using a nanodrop spectrophotometer (ND-1000, Nanodrop Technologies). In addition to nucleic acid measurements, the nanodrop instrument was used for measurements of protein contamination (the absorbance ratio at 260 nm/280 nm), and contamination with organic compounds (the absorbance ratio at 260 nm/230 nm). For the purpose of microarray analysis, the absorbance ratio of 260 nm/280 nm must be above 1.8, indicating relative RNA purity (**Table 1**).

RNA labeling

After RNA isolation from the samples, the miR-CURY™ Hy3™/Hy5™ Power labeling kit (Exiqon, Vedbaek, Denmark) was used according to the manufacturer's guidelines for miRNA labeling. One microgram of each sample was 3'-end-labeled with Hy3TM fluorescent label, using T4 RNA ligase and the following procedure: RNA in 2.0 μL of water was combined with 1.0 μL of CIP buffer and CIP (Exiqon). The mixture was incubated for 30 min at 37°C, and enzymatic activity was terminated by incubation for 5 min at 95°C. Then, 3.0 μL of labeling buffer, 1.5 μL of fluorescent label (Hy3TM), 2.0 μL of DMSO, and 2.0 μL of labeling enzyme were added into the mixture. The labeling reaction was incubated for 1 h at 16°C, and the reaction was terminated by incubation for 15 min at 65°C.

Array hybridization

Following the labeling procedure, the Hy3TM-labeled samples were hybridized on a miR-CURYTM LNA Array (v.16.0) (Exiqon) according to instructions. Briefly, the total 25 μL mixture

from the Hy3TM-labeled samples was mixed with 25 μL hybridization buffer, denatured for 2 min at 95°C, incubated on ice for 2 min and hybridized to the microarray for 16-20 h at 56°C in a 12-Bay Hybridization System (Hybridization System-Nimblegen Systems, Inc., Madison, WI, USA). Following hybridization, the slides were washed several times with buffer (Exiqon), and finally dried by centrifugation for 5 min at 400 rpm. Then the slides were scanned using the Axon GenePix 4000B microarray scanner (Axon Instruments, Foster City, CA).

Statistical analysis

Grid alignment and data extraction were performed using GenePix Pro 6.0 software (Axon). Replicated miRNAs were averaged. The expression levels of miRNAs with intensities > 30 in all samples were chosen as the normalization factor. Expression data were normalized using the Median normalization. After normalization, differentially expressed miRNAs were identified using student t-test and *p*-value < 0.05 was considered as significant.

Public domain databases

Information about the 1,881 human microRNAs was taken from the miRBase [15]. Experimentally validated miRNA-target interactions were taken from the miRTarBase [16]. Experimentally validated human protein-protein interactions (PPI) were taken from the Human Protein Reference Database (HPRD), release 9 [17].

Permutation test

Three miRNAs were randomly selected from the 1,249 human miRNAs in the array. The

Table 2. Target gene prediction

ID	Name	Target Gene
42576	hsa-miR-342-5p	AKR1B1, ANKRD12, ATRX, BCLAF1, CCNE1, DDX1, EIF3D, ELP3, FAM65A, GAPDH, KIF7, MCMBP, MMACHC, ND2, NFE2L1, NUFIP2, PHF17, PPIA, PRRC2C, PSMC1, PTPRG, RNPS1, ROBO2, SMARCA4, TBC1D22A, TMEM109, UCP3, USP36, VPS13D
148085	hsa-miR-3687	KIAA0355, PPARGC1B, RAI1
42866	hsa-miR-451a	ABCB1, AKT1, ARPP19, BCL2, CAB39, MIF, MMP2, MMP9, MYC, RAB14, TMED7, UBE2H
31076	hsa-miR-559	ERBB2, FXN, MTA1, MTA2, VCL
42960	hsa-miR-513a-3p	GSTP1, CD274

Table 3A. T vs C 2.0 fold up regulated miRNAs

ID	Name	Fold change	P-value
		T vs C*	T vs C
42576	hsa-miR-342-5p	3.416724	0.020657
148085	hsa-miR-3687	17.35892	0.002397
42866	hsa-miR-451a	2.777202	0.023158

MiRNAs defined as differentially up-regulated in miRNA microarray analysis only when the fold changes of T over C ≥ 2.0. *T: the experimental group; C: the control group.

miRNA associated protein-protein interaction (PPI) sub-network of these three selected miRNAs was constructed and tested to identify sub-network connections between the three selected miRNAs. A million cycles of random selection from the three miRNAs were conducted. The false discovery rate was estimated as the total amount of connected sub-networks divided by a million.

Gene enrichment analysis

Two types of enrichment analyses were performed on the genes mediated by significantly up- or down-regulated miRNAs: the transcription factor enrichment analysis and the disease-associated gene enrichment analysis. The transcription factor enrichment analysis was performed using the ChIP Enrichment Analysis found on the website ChEA2 (website: http://amp.pharm.mssm.edu/ChEA2) [18]. The disease-associated gene enrichment analysis was performed on the Enricher based on the NCBI Online Mendelian Inheritance in Man (OMIM) database [19, 20].

Results

Differentially expressed miRNAs in UPJO

In order to decipher the mechanism of disease at the mRNA post-transcription regulation level, differentially expressed miRNAs between cases of UPJO and control samples were identified. There were five miRNAs differentially expressed ($P < 0.05$) between case samples and control samples. Three of these microRNAs were consistently found to be up-regulated (**Table 3A**): hsa-mir-451a, hsa-mir-342-5p, and hsa-mir-3687. Conversely, three of these microRNAs were found to be down-regulated: hsa-miR-559, hsa-miR-513a(c)-3p, and kshv-miR-K12-1-3p (**Table 3B**). Among which, kshv-miR-K12-1-3p was not a human miRNA and therefore would not be considered as a potential biomarker of UPJO in children.

Target prediction

In fact, miRNA is involved in the process of post-transcriptional regulation, we determine to prove whether there was some correlation between the expression levels of miRNAs and their target genes involved in the pathogenesis of UPJO. Target prediction was performed for miRNAs by using 4 Databases (miRTarBase, HPRD TargetScan, and miRDB) to identify the genes, based on the similar prediction by no less than 3 of the 4 databases. Official symbol of miRNA, such as hsa-mir-342-5p, was used to map between databases. There were 44 genes mediated by three significantly up-regulated miRNAs and seven genes mediated by two significantly down-regulated miRNAs (**Table 2**).
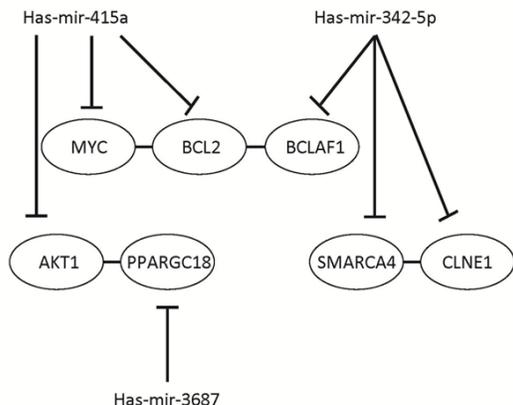
Protein-protein interactions network constructed by the differentially expressed miRNAs

Expressed mRNAs are translated into proteins. One of the major mechanisms of protein function is interaction with other proteins. As a consequence, investigating the protein-protein interaction network may reveal some roles of differentially expressed miRNAs at the transcriptional regulation level. Each miRNA-associated PPI network was constructed using miRNAs, the corresponding target genes of the

Table 3B. T vs C 2.0 fold down regulated miRNAs

| ID | Name | Fold change | P-value |
		T vs C	T vs C
147831	kshv-miR-K12-1-3p	0.245972	0.035199
31076	hsa-miR-559	0.438787	0.015915
42960	hsa-miR-513a-3p/hsa-miR-513c-3p	0.284495	0.017013

MiRNAs are defined as differentially down-regulated in the miRNA microarray analysis only when the fold changes of T over C ≤ 0.5.

Figure 2. Micro RNA associated protein-protein interaction network. Three microRNAs were up-regulated in the case group and were connected together through *AKT1, BCL2, PPARGC1B,* and *BCLAF1*.

miRNAs, and the interaction partners of target genes. The target genes of three up-regulated miRNAs were connected together (**Figure 2**). No protein-protein interaction network was found between targeted genes of two of the down-regulated miRNAs.

Three up-regulated miRNAs repress the Akt/ mTOR signaling pathway

Up-regulated miRNAs may be associated with each other through co-repression genes that work together, such as in a sub PPI network or in a pathway. In this study, three up-regulated miRNAs-hsa-mir-451a, hsa-mir-342-5p, and hsa-mir-3687-were connected together through a PPI sub-network build by *AKT1, BCL2, PPARGC1B,* and *BCLAF1* (**Figure 2**). This miRNA-associated PPI network may imply that the Akt/mTOR signaling pathway was repressed through the down-regulation of *AKT1* and *BCL2* family (*BCL2* and *BCLAF1*), and simultaneously by up-regulation of three miRNAs-hsa-mir-451a, hsa-mir-342-5p, and hsa-mir-3687-in

ureteral-pelvic junction obstruction.

False discovery rate estimation

To test whether this connected network, constructed by three differentially up-regulated miRNAs, was purely random or not, the probability (termed the false discovery rate) of a connected network was constructed with the use of three random miRNAs. To evaluate the false discovery rate of this connected miRNA-associated PPI network, random permutations were performed to estimate the probability of a connected PPI network that could be found from three randomly selected miRNAs. After a million permutations, there were only 44,129 miRNA random combinations that could be found in a connected PPI network. The false discovery rate was 0.0441; thus, that the probability of seeing a connected PPI network constructed by three randomly selected miRNAs was only 4.41%.

Gene enrichment analysis

Gene enrichment analyses were used to detect the over-representation of genes in the specific events such as diseases, pathways, or ontology. In this study, we performed two types of gene enrichment analyses. One was the transcription factor enrichment analysis. This analysis detects transcription factors which also regulate genes targeted by the three differentially up-regulated miRNAs. The other was the disease-associated gene enrichment analysis, which was used to identify the diseases most likely associated genes targeted by the three differentially up-regulated miRNAs.

In the transcription factor enrichment analysis, 44 genes mediated by the three significantly up-regulated miRNAs were analyzed on the ChEA2. Two transcription factors, RUNX1 (P = 3.337e-11) and FLI1 (P = 5.721e-10), were most significantly associated with our gene list. Both *RUNX1* and *FLI1* were associated with white blood cell diseases. In the disease-associated gene enrichment analysis, the gene list was sent to the Enrichr website. Two genes, *MYC* and *BCL2*, were found to be associated with lymphoma (P = 0.004712).

Discussion

In this study, five differentially expressed miRNAs were identified through a comprehensive comparison of miRNA expression profiles between case and control groups. These miRNAs are potential biomarkers of UPJO in children. Bioinformatics analyses of these differentially expressed miRNAs further showed that three up-regulated miRNAs were associated with each other through a PPI sub-network. Enrichment analysis showed that the genes targeted by the three up-regulated miRNAs were generally associated with lymphoma and were also regulated by two transcription factors associated with white blood cell diseases.

More experiments at other molecular levels should be done to study the detailed mechanisms of these associations, such as yeast-two-hybrid, ChIP-seq, and expression chip in the future.

The Akt/mTOR pathway is considered to be an important anti-apoptotic signal for cell survival. Damage in cells may activate the apoptosis signaling pathway thus lead to renal cell apoptosis in children with UPJO. Results from our analysis implied that the observed apoptosis may be associated with silencing of the Akt/mTOR signaling through up-regulation of the three miRNAs we identified. The false discovery rate was only 4.41%, implying that the PPI network identified by the three up-regulated miRNAs were not a random event.

Transcription factors and microRNAs are the two major molecules controlling gene expression at the mRNA level. An exploration of the roles of transcription factors which may be involved in the regulation of the genes we identified may provide more information about these genes. In other words, while we have only limited knowledge about candidate miRNAs, exploration of transcription factors that regulate similar genes may provide some insight. Disease-associated gene enrichment analysis provided some insight into the roles of genes regulated by miRNAs. Diseases from similar sources, involving similar pathways, or causing similar physiological phenotypes may involve similar genes.

In this study, we found BCL2 may be repressed by hsa-mir-415 and by the other two up-regulat-

ed miRNAs through which the mTOR/AKT pathway may be repressed. Since BCL2 is an anti-apoptotic protein, decreased expression of BCL2 may lead to apoptosis or cell death in the patient with UPJO. During obstruction, inflammation and oxidative stress may induce a severe apoptotic response of both tubular and interstitial cells. Our findings are consistent with other studies reporting decreased expression of BCL2 as a signature of UPJO in the animal model [21, 22]. We suggest that downregulation of BCL2 may be caused by the increased expression of hsa-mir-415.

In the clinical settings, detecting increased expression of presumptive genes may be more useful than detecting decreased expression of these genes. If the relationship between hsa-mir-415 and BCL2 expression is confirmed in patients with UPJO, hsa-mir-415 may be a potential biomarker for detecting early UPJO. In combination with the other two up-regulated miRNAs we identified, a multi-gene signature of early UPJO may increase the accuracy and precision of early UPJO detection and lead to more effective treatments for this disease.

Disclosure of conflict of interest

None.

Address correspondence to: Dr. Li Zhou, Department of Pediatric Surgery, First Affiliated Hospital, University of Sun Yat-sen, Guangzhou 510080, Guangdong, China. Tel: 86-20-87755766-8118; E-mail: ligdhzhou@163.com

References

[1] Chevalier RL, Thornhill BA, Forbes MS and Kiley SC. Mechanisms of renal injury and progression of renal disease in congenital obstructive nephropathy. Pediatr Nephrol 2010; 25: 687-697.

[2] Garne E, Loane M, Wellesley D, Barisic I; Eurocat Working Group. Congenital hydronephrosis: Prenatal diagnosis and epidemiology in Europe. J Pediatr Urol 2009; 5: 47-52.

[3] Botto N, Azoulay R, Peuchmaur M and El Ghoneimi A. Renal parenchymal fibrosis and atrophy are not correlated with upper tract dilatation: Long-term study of partial unilateral ureteral obstruction in neonatal mice. J Pediatr Urol 2011; 7: 310-316.

[4] Piepsz A, Gordon I, Brock J and Koff S. Round table on the management of renal pelvic dila-

tation in children. J Pediatr Urol 2009; 5: 437-444.

[5] Chevalier RL and Peters CA. Congenital urinary tract obstruction: Proceedings of the State-Of-The-Art Strategic Planning Workshop-National Institutes of Health, Bethesda, Maryland, USA, 11-12 March 2002. Pediatr Nephrol 2009; 18: 76-606.

[6] Chandrasekaran K, Karolina DS, Sepramaniam S, Armugam A, Wintour EM, Bertram JF and Jeyaseelan K. Role of microRNAs in kidney homeostasis and disease. Kidney Int 2012; 81: 617-627.

[7] Chung AC, Huang XR, Meng X and Lan HY. miR-192 mediates TGF-β/Smad3-driven renal fibrosis. J Am Soc Nephrol 2010; 21: 1317-1325.

[8] Denby L, Ramdas V, McBride MW, Wang J, Robinson H, McClure J, Crawford W, Lu R, Hillyard DZ, Khanin R, Agami R, Dominiczak AF, Sharpe CC and Baker AH. miR-21 and miR-214 are consistently modulated during renal injury in rodent models. Am J Pathol 2011; 179: 661-672.

[9] Qin W, Chung AC, Huang XR, Meng XM, Hui DS, Yu CM, Sung JJ and Lan HY. TGF-β/Smad3 signaling promotes renal fibrosis by inhibiting miR-29. J Am Soc Nephrol 2011; 22: 1462-1474.

[10] Oba S, Kumano S, Suzuki E, Nishimatsu H, Takahashi M, Takamori H, Kasuya M, Ogawa Y, Sato K, Kimura K, Homma Y, Hirata Y and Fujita T. miR-200b precursor can ameliorate renal tubulointerstitial fibrosis. PLoS One 2010; 5: e13614.

[11] Xiong M, Jiang L, Zhou Y, Qiu W, Fang L, Tan R, Wen P and Yang J. The miR-200 family regulates TGF-β1-induced renal tubular epithelial to mesenchymal transition through Smad pathway by targeting ZEB1 and ZEB2 expression. Am J Physiol Renal Physiol 2012; 302: F369-F379.

[12] Kriegel AJ, Liu Y, Cohen B, Usa K, Liu Y and Liang M. MiR-382 targeting of kallikrein 5 contributes to renal inner medullary interstitial fibrosis. Physiol Genomics 2012; 44: 259-267.

[13] Bai XY, Ma Y, Ding R, Fu B, Shi S and Chen XM. miR-335 and miR-34a promote renal senescence by suppressing mitochondrial antioxidative enzymes. J Am Soc Nephrol 2011; 22: 1252-1261.

[14] Sui W, Dai Y, Huang Y, Lan H, Yan Q, Huang H. Microarray analysis of MicroRNA expression in acute rejection after renal transplantation. Transpl Immunol 2008; 19: 81-85.

[15] Kozomara A and Griffiths-Jones S. miRBase: annotating high confidence microRNAs using deep sequencing data. Nucleic Acids Res 2013; 42: D68-D73.

[16] Hsu SD, Tseng YT, Shrestha S, Lin YL, Khaleel A, Chou CH, Chu CF, Huang HY, Lin CM, Ho SY, Jian TY, Lin FM, Chang TH, Weng SL, Liao KW, Liao IE, Liu CC and Huang HD. miRTarBase update 2014: an information resource for experimentally validated miRNA-target interactions. Nucleic Acids Res 2014; 42: D78-D85.

[17] Keshava Prasad TS, Goel R, Kandasamy K, Keerthikumar S, Kumar S, Mathivanan S, Telikicherla D, Raju R, Shafreen B, Venugopal A, Balakrishnan L, Marimuthu A, Banerjee S, Somanathan DS, Sebastian A, Rani S, Ray S, Harrys Kishore CJ, Kanth S, Ahmed M, Kashyap MK, Mohmood R, Ramachandra YL, Krishna V, Rahiman BA, Mohan S, Ranganathan P, Ramabadran S, Chaerkady R and Pandey A. Human protein reference database-2009 update. Nucleic Acids Res 2009; 37 Suppl 1: D767-D772.

[18] Kou Y, Chen EY, Clark NR, Duan Q, Tan CM and Ma'ayan A. ChEA2: Gene-set libraries from ChIP-X experiments to decode the transcription regulome. In: Cuzzocrea A, et al, editors. Availability, Reliability, and Security in Information Systems and HCI. Heidelberg Berlin: Springer; 2013. pp. 416-430.

[19] Chen EY, Tan CM, Kou Y, Duan Q, Wang Z, Meirelles GV, Clark NR and Ma'ayan A. Enrichr: interactive and collaborative HTML5 gene list enrichment analysis tool. BMC Bioinformatics 2013; 14: 128.

[20] McKusick-Nathans Institute of Genetic Medicine, J.H.U.B., MD), Online Mendelian Inheritance in Man, OMIM®. World Wide Web URL: http://omim.org/. 2014.

[21] Yoo KH, Thornhill BA, Forbes MS and Chevalier RL. Inducible nitric oxide synthase modulates hydronephrosis following partial or complete unilateral ureteral obstruction in the neonatal mouse. Am J Physiol Renal Physiol 2010; 298: F62-F71.

[22] Klein J, Gonzalez J, Miravete M, Caubet C, Chaaya R, Decramer S, Bandin F, Bascands JL, Buffin-Meyer B and Schanstra JP. Congenital ureteropelvic junction obstruction: human disease and animal models. Int J Exp Pathol 2011; 92: 168-192.